A Concept for Earthquake-Resistant Design of Underground Structures: Stress Response Spectrum

Ayumi Kurose, Pierre Bérest

A concept for earthquake-resistant design of underground structures: Stress response spectrum

Ayumi Kurose & Pierre Berest
Laboratoire de Mécanique des Solides, Ecole Polytechnique, Palaiseau, France

ABSTRACT: This paper introduces a method to evaluate the mechanical effects induced in the cross-section of an underground structure, constructed in a medium of great thickness, under earthquake ground motion. Damage observations after large earthquakes (e.g., Kobe, 1995) have shown the cross-sectional vulnerability of underground structures at shallow or great depth. Present earthquake-resistant design standards only suggest calculation methods for structures constructed in a soil laying over a rigid basement and cannot be applied to a structure constructed in a medium of great thickness, such as a tunnel, an underground hydrocarbon storage facility or a nuclear-waste disposal site. Thus, development of a systematic method to evaluate the seismic effects induced in the cross-section of a structure in an unbounded medium is of interest. The approach proposed here is conceptually similar to that used for earthquake response analysis of buildings: using a simple but realistic model of an underground linear structure (a 2D cavity with circular cross-section in an infinite, elastic, linear, homogeneous and isotropic medium) and real earthquake records, we propose a response spectrum more suitable, than the usual velocity or acceleration response spectrum, for analyzing the structural stability of underground construction during earthquakes: the *Stress Response Spectrum* (*SRS*), which is defined as the maximum value of the maximum shear stress at the cavity wall during the duration of ground motion. The *SRS* values are computed by using 21 earthquake motions (provided by the Japan Meteorological Agency) of magnitude higher than 4, which were recorded by the Japan Nuclear Cycle Research Institute (JNC) in a 315-meter deep gallery excavated in an a granodioritic rock mass at the Kamaishi Mine in Iwate, Japan. In light of the numerical analysis, the *SRS* appears to be a potential tool for the earthquake-response analysis of underground structures. The Stress Response Spectrum will provide engineers with the order of magnitude of mechanical effects in an underground structure for a given earthquake motion; conversely, for a given target *SRS*, may assist in producing a design earthquake more suitable for analysis of deep underground structures than those currently available.

1 INTRODUCTION

Damage observed after large earthquakes shows the vulnerability of underground structures in their cross-sections. During the January 17, 1995 Hyogo-ken Nanbu earthquake, several lined mountain tunnels having an overburden of several hundred meters seem to have suffered significantly from the dynamic deformation of the surrounding medium (Fig.1, (Sakurai 1995)).

With regard to the evaluation of earthquake-related mechanical effects in the cross-section, present earthquake-resistant design standards only suggest methods for structures constructed in a soil laying over a rigid basement (Fig.2, (Kawashima 1994)) on which a horizontal acceleration $\ddot{u}_B$ is applied. This rigid basement model cannot explain the damage in

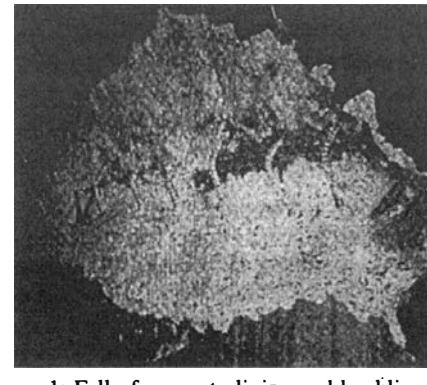

Figure 1: Fall of concrete lining and buckling of the reinforcing bars, Bantaki tunnel, Kobe [After Sakurai, 1995].

compression shown in Fig.1 or be applied to a structure constructed in a medium of great thickness, such as an underground hydrocarbon storage facility or a nuclear waste disposal site. Thus, development of a systematic method to evaluate seismic effects induced in the cross-section of a structure in an unbounded medium is needed.

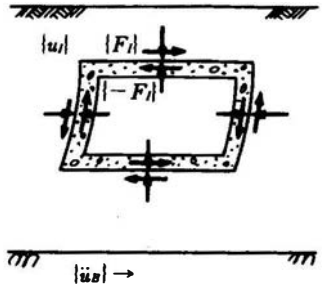

Figure 2: Soil-structure interaction [after Kawashima, 1994]

2 PHILOSOPHY

The proposed approach is similar to that first used to develop earthquake-resistant design methods for buildings, the major concept of which is the *response spectrum*. The response spectrum is the maximum response in velocity or acceleration to a given ground motion of a series of single-degree-of-freedom (SDOF) systems characterized by a fundamental period and a damping coefficient. This concept plays an important role in current design methods for buildings.

Similarly, we propose to use a simple but realistic model of an underground linear structure, such as a tunnel, to define three notions: (i) a characteristic period of the structure; (ii) a physical parameter that measures the vulnerability of the structure (stress); and (iii) a response spectrum suited to the analysis of the structural stability of underground construction (stress response spectrum).

3 MODEL FOR UNDERGROUND STRUCTURES

A simple model for underground structures can never be as simple as an SDOF system. The model considered here is an unlined 2D cavity with circular cross-section, of radius a, in an infinite, elastic, homogeneous and isotropic medium characterized by density, ρ, and shear velocity, c_s. The structure is subjected to an incident SH plane wave propagating upward ($x1 > 0$, see Fig.3). This is, relatively to the cross-section, an anti-plane problem, with the incident displacement,which is z-independent and expressed by $\underline{u}^{inc} = w^{inc}(r,\theta)\underline{e}_z$.

For simplicity, an incident SH-wave, rather than a P- or SV-wave, is used in this paper, because incident SH-waves generate SH-diffracted waves only, thus maintaining the anti-plane nature of the problem.

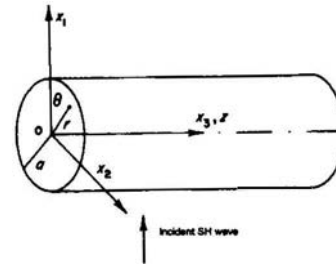

Figure 3: Study model

4 TYPE OF INCIDENT MOVEMENT

Case 1: As an academic example of our approach, a study using monochromatic plane-wave incidence is proposed to expound relevant mechanical fields and concepts, such as the characteristic period of the cavity, T_c. An application is suggested for a preliminary earthquake-resistant design analysis of an underground linear structure.

Case 2: To understand the co-seismic behavior of the cavity, analyses using real earthquake records are needed. In keeping with the hypothesis of plane wave, a simple computational method, using the formulae of monochromatic wave study and sampling theory, is suggested for evaluating the stresses around the cavity. This enables definition of the most important concept developed in this paper: the *Stress Response Spectrum* (*SRS*), equivalent to the response spectrum used in building earthquake-resistant design.

5 CASE 1: MONOCHROMATIC WAVE INCIDENCE

5.1 MECHANICAL ANALYSIS

In light of Pao and Mow's 1973 study (Pao & Mow 1973), the incident displacement w^{inc} is defined in Cartesian or polar coordinates as:

$$w^{inc} = w_0 \exp[i(\beta x - \omega t)]$$

$$= w_0 \sum_{n=0}^{\infty} \varepsilon_n i^n J_n(\beta r)\cos n\theta \exp(-i\omega t) \quad (1)$$

with $\varepsilon_0 = 1$ and $\varepsilon_n = 2, n \geq 2$; J_n is the Bessel function of the first kind of order n, ω is the circular frequency, and $\beta = \omega a/c_s$ is the shear wave number.

The form of the diffracted displacement, w^{dif}, is chosen to satisfy the scalar Helmholtz equation, $\Delta w + (\omega^2/c_s^2)w = 0$. Thus,

$$w^{dif} = w_0 \sum_{n=0}^{\infty} \varepsilon_n i^n A_n H_n^{(1)}(\beta r)\cos n\theta \exp(-i\omega t) \quad (2)$$

where $H_n^{(1)}$ is the Hankel function of the first kind of order n.

The non-zero mechanical fields are the total displacement ($u_z = w^{inc} + w^{dif}$), and the stress components σ_{rz} and $\sigma_{\theta z}$. Using Pao and Mow's notations:

$$u_z = w_0 \sum_{n=0}^{\infty} \varepsilon_n i^n [J_n(\beta r) + A_n H_n^{(1)}(\beta r)] \cos n\theta \exp(-i\omega t) \quad (3)$$

$$\sigma_{rz} = \frac{\rho c_s^2 w_0}{r} \sum_{n=0}^{\infty} \varepsilon_n i^n [E_{82}^{(1)}(n,\beta r) + A_n E_{82}^{(3)}(n,\beta r)] \cos n\theta \exp(-i\omega t) \quad (4)$$

$$\sigma_{\theta z} = -\frac{\rho c_s^2 w_0}{r} \sum_{n=0}^{\infty} \varepsilon_n i^n [E_{72}^{(1)}(n,\beta r) + A_n E_{72}^{(3)}(n,\beta r)] \sin n\theta \exp(-i\omega t) \quad (5)$$

with

$$E_{82}^{(1)}(n,\beta r) = \beta r J_{n-1}(\beta r) - n J_n(\beta r) \quad (6)$$

$$E_{82}^{(3)}(n,\beta r) = \beta r H_{n-1}^{(1)}(\beta r) - n H_n^{(1)}(\beta r) \quad (7)$$

$$E_{72}^{(1)}(n,\beta r) = n J_n(\beta r) \quad (8)$$

$$E_{72}^{(3)}(n,\beta r) = n H_n^{(1)}(\beta r) \quad (9)$$

Coefficients A_n are determined from the stress-free condition on the cavity wall: $\sigma_{rz}(r = a) = 0$, which yields:

$$A_n = -E_{82}^{(1)}(n,\beta a)/E_{82}^{(3)}(n,\beta a) \quad (10)$$

Incident velocity, v^{inc}, is the time derivative of w^{inc}. Using Eq.(1), we obtain: $v^{inc} = v_0 \exp[i(\beta x - \omega t)]$, with

$$v_0 = -i\omega w_0 \quad (11)$$

Using this expression of v_0 in Eq.(5), stress component $\sigma_{\theta z}$ can be expressed as:

$$\sigma_{\theta z} = \rho c_s v_0 \mu_{sh}(\beta a, \beta r, \theta) \exp(-i\omega t) \quad (12)$$

with

$$\mu_{sh}(\beta a, \beta r, \theta) = \frac{1}{i\beta r} \sum_{n=0}^{\infty} \varepsilon_n i^n [E_{72}^{(1)}(n,\beta r) + A_n E_{72}^{(3)}(n,\beta r)] \sin(n\theta) \quad (13)$$

Function μ_{sh} is a reminder of Mow and Pao's *dynamic stress concentration factor*. Here, we define a characteristic period of the cavity,

$$T_c = a/c_s \quad (14)$$

which characterizes the cavity-medium interaction. If function μ_{sh} is evaluated at the cavity wall (r = a), where maximum stress is expected, we notice that this function depends on the incident motion and the structure only via products $\beta a = \omega T_c$ and θ. The usual value of T_c is between 10^{-3} s and 10^{-2} s. Fig.4 shows the maximum amplitudes of μ_{sh} at the cavity wall ($r = a$):

$$\max_{\theta\in[0,2\pi]} |\mu_{sh}(\omega T_c, \omega T_c, \theta)| = \max_{\theta\in[0,2\pi]} \left(\left| \frac{\sigma_{\theta z}}{\rho c_s v_0} \right| \right) \quad (15)$$

as functions of T_c and incident wave frequency, f_0.

For low values of f_0 ($f_0 < 0.2$Hz), the maximum amplitudes are slightly dependent on T_c ($T_c < 0.02$s). The peak values of about 2.1 occur for $T_c \simeq 0.06/f_0$, and are less than 10% higher than the values for $T_c \simeq 0$. These conclusions are similar to those of Mow and Pao. In Fig.(4), we notice a complex variation of curves between $f_0 = 2$Hz and 5Hz, which is the relevant frequency interval for earthquake engineering. Note that, at $r = a$, with given ω,

$$\lim_{T_c \to 0} \mu_{sh}(\omega T_c, \omega T_c, \theta) = 2\sin\theta \quad (16)$$

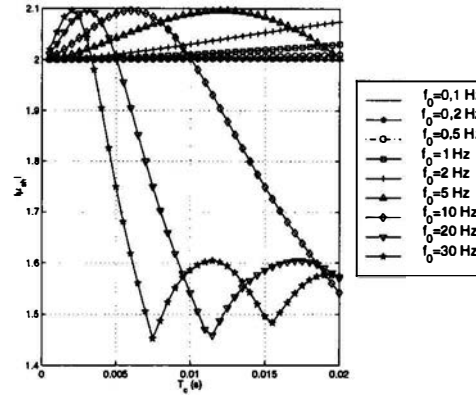

Figure 4: Maximum amplitude of μ_{sh} at $r = a$

5.2 APPLICATION

For a preliminary earthquake-resistant design analysis, we can determine a fundamental period f_0 (Rathje et al. 1998) and the peak velocity v_0 (Betbeder-Matibet 1999) of the expected earthquake motion at the target underground site from the seismo-tectonic context and an earthquake-design regulation code or empirical study. If c_s is known, the critical radius, a_c, for which the peak stress occurs at frequency f_0, is:

$$a_c = 0.06 c_s / f_0 \tag{17}$$

Thus, from the seismic viewpoint, it is better to design a cavity of radius either smaller or much larger than a_c (see Fig.4).

If the fundamental period of the site is assumed to be $f_0 = 5$Hz and the peak velocity is $|v_0| = 0.05$m/s, the maximum stress around the cavity occurs for $T_c = a_c/c_s \simeq 0.012$s.

The peak amplitude of the dynamic stress component, $\sigma_{\theta z}$, at the cavity wall, is obtained from Eq.(12) and is, with $\rho = 2600\text{kg/m}^3$, about 0.3 MPa for $a_c \simeq 14$m, if $c_s = 1200$m/s, and about 0.9 MPa for $a_c \simeq 36$m, if $c_s = 3000$m/s.

6 CASE 2: EARTHQUAKE MOTION

6.1 MECHANICAL ANALYSIS

Theoretically, earthquake records give the time-sampled values of acceleration, velocity and displacement, from which the corresponding Fourier transform can be computed. If we consider that (i) the incident wave is a recorded motion; (ii) at $x = 0$, the incident displacement is $w_0[m]$, $m = 1..N$, where N is the total number of data points sampled with timestep T (the corresponding Fourier amplitude is noted $w_0[k]$, $k = 1..N$); and (iii) the hypothesis of plane-wave propagation is maintained, then the displacement Fourier amplitude at point x is given by $w_0[k]\exp(i\beta_k x) = \sum_{n=0}^{\infty} \varepsilon_n i^n J_n(\beta_k r)\cos n\theta$, with $\beta_k = \omega_k/c_s = 2\pi k/(NTc_s)$. Using the preceding analysis for monochromatic waves (Section 5.1: CASE 1), the frequency-sampled mechanical fields can be given by:

$$u_z[k,r,\theta] = w_0[k] \sum_{n=0}^{\infty} \varepsilon_n i^n \tag{18}$$

$$[J_n(\beta_k r) + A_n[k] H_n^{(1)}(\beta_k r)]\cos n\theta$$

$$\sigma_{rz}[k,r,\theta] = \frac{\rho c_s^2 w_0[k]}{r} \tag{19}$$

$$\sum_{n=0}^{\infty} \varepsilon_n i^n [E_{82}^{(1)}(n,\beta_k r) + A_n[k] E_{82}^{(3)}(n,\beta_k r)]\cos n\theta$$

$$\sigma_{\theta z}[k,r,\theta] = -\frac{\rho c_s^2 w_0[k]}{r} \tag{20}$$

$$\sum_{n=0}^{\infty} \varepsilon_n i^n [E_{72}^{(1)}(n,\beta_k r) + A_n[k] E_{72}^{(3)}(n,\beta_k r)]\sin n\theta$$

The stress-free condition at $r = a$ for indices n and k gives:

$$A_n[k] = -E_{82}^{(1)}(n,\beta_k a)/E_{82}^{(3)}(n,\beta_k a) \tag{21}$$

Thus, with $v_0[k] = -i\omega_k w_0[k]$ and $\beta_k a = \omega_k T_c$, at $r = a$, Eq.(21) yields

$$\sigma_{\theta z}[k,\rho,c_s,T_c,\theta] = \rho c_s v_0[k] \mu_{sh}(\omega_k T_c, \omega_k T_c, \theta) \tag{22}$$

and its inverse Fourier transform, $\sigma_{\theta z}[m,\rho,c_s,T_c,\theta]$, corresponds to the time-sampled stress component around the cavity if the surrounding medium is infinite, elastic, linear, isotropic and homogeneous. The introduction of velocity amplitude, v_0, instead of displacement, w_0, in Eqs.(12), (22) has two advantages: (i) it singles out the part related to the site conditions (ρ, c_s) from the geometrical parameters in function μ_{sh}; and (ii) it avoids several time integrations of earthquake motion usually recorded in acceleration or velocity. (Those integrations introduce additional errors.)

6.2 DEFINITION OF STRESS RESPONSE SPECTRUM

In rock-mechanics design, the determination of the maximum shear stress is useful for analyzing structural stability.

At $r = a$, the real dynamic stress tensor in the medium is $\underline{\underline{\sigma}}^{dyn} = \Re(\sigma_{\theta z})(\underline{e_z} \otimes \underline{e_\theta} + \underline{e_\theta} \otimes \underline{e_z})$, and the time-sampled maximum shear stress, evaluated at $r = a$, is:

$$\tau_{max}[m,\rho,c_s,T_c,\theta] = |\Re(\sigma_{\theta z}[m,\rho,c_s,T_c,\theta])| \tag{23}$$

Here, we define the stress response spectrum (*SRS*) as the maximum value of τ_{max} in time at $r = a$:

$$SRS(\rho,c_s,T_c) \stackrel{def}{=} \max_{m,\theta}\{\tau_{max}[m,\rho,c_s,T_c,\theta]\} \tag{24}$$

The *SRS* is a function of characteristic period $T_c = a/c_s$ and corresponds to the peak dynamic shear stress. Through Mohr-Coulomb analysis, the increment of static shear stress by the *SRS* for a given T_c enables the distance from failure to be evaluated.

Note that, at $r = a$, with given index k, Eqs.(16) and (22) yield

$$\lim_{T_c \to 0} \sigma_{\theta z}[k,\rho,c_s,T_c,\theta] = 2\rho c_s v_0[k]\sin\theta \tag{25}$$

Thus, for $T_c = 0$ s, the inverse Fourier transform of stress component $\sigma_{\theta z}$ is expressed as

$$\sigma_{\theta z}[m, \rho, c_s, T_c = 0, \theta] = 2\rho c_s v_0[m] \sin\theta \qquad (26)$$

and the *SRS*, according to formula (24), is

$$SRS(\rho, c_s, T_c = 0) = 2\rho c_s v_M \qquad (27)$$

where $v_M = \max_m\{v_0[m]\}$ is the maximum value, in time, of the earthquake velocity.

6.3 EARTHQUAKE INPUT

A total of 21 earthquake motions are used to compute the normalized $SRS/(\rho c_s v_M)$ values. They were recorded from 1988 to 1998 by the Japan Nuclear Cycle Research Institute (JNC) in a 315-meter deep gallery in a granodioritic rock mass at the Kamaishi Mine in Iwate, Japan. The motions correspond to earthquakes for which the maximum acceleration measured at a depth of 615 meters were higher than 2 cm/s^2. Among the 21 earthquakes, the JNC considers 15 motions to have been generated by ruptures at the subduction zones (interplate earthquakes, group 1) and 6 earthquakes to have been intraplate earthquakes (group 2). Table 1 shows the number of earthquakes used for the *SRS* computation as a function of magnitude provided by the Japan Meteorological Agency, and the computed mean velocity for each case. The epicentral distances range from 41 km to 460 km for group 1, and from 12 km to 53 km for group 2.

Table 1: Earthquakes used for the *SRS* computation

Magnitude	Group 1		Group 2	
	No	V_{mean} (cm/s)	No	V_{mean} (cm/s)
$4 < M \leq 5$ (Fig.5)	5	0.1	3	0.3
$5 < M \leq 6$ (Fig.6)	4	0.3	3	0.3
$6 < M \leq 7$ (Fig.7)	3	0.5	0	×
$7 < M$ (Fig.7)	3	1.7	0	×

6.4 NUMERICAL ANALYSIS

6.4.1 Examples of *SRS*

The normalized values, $SRS/(\rho c_s v_M)$, are computed as functions of T_c, varying from 0.0005 s to 0.02 s with step 0.0005 s and magnitude M. They are shown in Figs.5 to 7, corresponding to the cases mentioned in Tab.1. As seen, the difference in cavity stress responses to given earthquakes varies according to their magnitude. The amplitudes of spectral variations decrease with magnitude range. The decrease of *SRS* values for high T_c is more remarkable for $4 < M \leq 5$ than for $5 < M \leq 6$; for magnitudes higher than 6, the normalized *SRS* has a nearly constant value of 2 whatever the T_c and ground motions are.

Using the rock data from the Kamaishi Mine ($c_s = 3000$m/s, $\rho = 2600$kg/m^3) and the mean velocity values of ground motion in Table 1, the maximum *SRS* values are about 0.05 MPa for $4 < M \leq 6$, 0.08 MPa for $6 < M \leq 7$, and 0.3 MPa for $7 < M$.

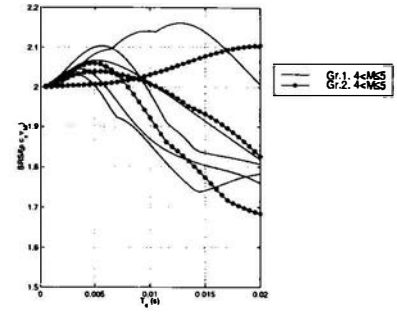

Figure 5: Normalized *SRS*: gr.1 and 2 ($4 < M \leq 5$)

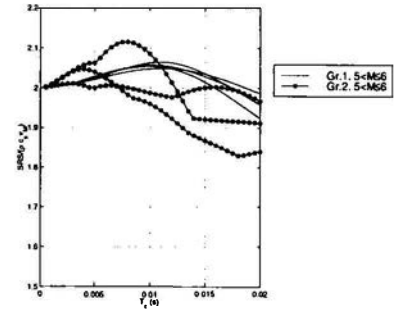

Figure 6: Normalized *SRS*: gr.1 and 2 ($5 < M \leq 6$)

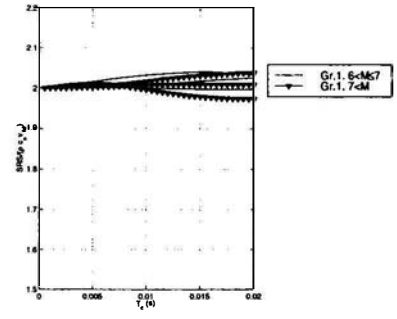

Figure 7: Normalized *SRS*: gr.1 ($6 < M$)

6.4.2 Monochromatic Wave versus Earthquake Motion

An example comparison of cavity stress response to incident monochromatic wave and earthquake ground motion is shown in Fig.8.

The amplitudes of function μ_{sh} are computed using Eq.(15) for frequencies $f_0 = 8$Hz, 9Hz, 10Hz, and the normalized *SRS* values. Fig.9 shows the Fourier acceleration amplitude of the earthquake recorded at the Kamaishi Mine used to obtain the normalized *SRS* in Fig.8.

It can be seen from Fig.8 that, for low T_c, the *SRS* and μ_{sh} curves have similar slopes, corresponding to the curve computed for a monochromatic wave of $f_0 \simeq$ 9Hz in the above case. This indicates that a 2D circular cavity of low T_c can be expected to be sensitive to a certain period that does not necessarily correspond to the fundamental period of ground motion, as shown in Fig.9. For high T_c, there is no obvious correlation between the response to monochromatic waves and earthquake motion: the earthquake response of cavities with high T_c depends on the frequency content of the ground velocity.

Thus, a preliminary study using an incident monochromatic wave, as shown in section 5.2, has to be handled with care.

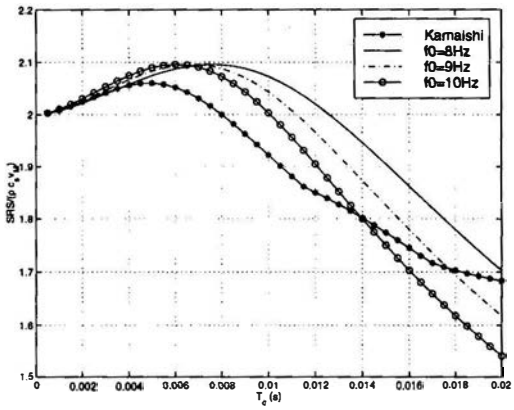

Figure 8: Comparison between monochromatic wave and earthquake inputs

7 CONCLUSIONS

A response analysis of unlined 2D cavities with circular cross-section under incident SH plane waves propagating in an infinite, elastic, linear, homogeneous and isotropic medium is carried out. The preliminary study of incident monochromatic waves gives information about the form of the stress fields around the cavity and the characteristic period of the cavity, T_c. Using this study and sampling theory, a simple computational method is proposed for evaluating the stress fields induced by real earthquake records, around a cavity. From time-sampled stresses, we define the concept of the Stress Response Spectrum (*SRS*) as a function of T_c and earthquake motion — that is, the maximum value of maximum shear stress τ_{max} in time at the cavity wall. The *SRS* values are computed from 21 earthquake ground motions that have been recorded by the JNC in a 315-meter deep granodioritic rock mass at the Kamaishi Mine in Iwate, Japan. The numerical analysis suggests the *SRS* to be a potential tool for study of earthquake response of underground structures according to seismological parameters, such as magnitude. *SRS* curves from more earthquake records with higher motion amplitudes are needed to determine the general trends of those curves as functions of seismological or geological parameters and to understand the correlation between the frequency content of ground velocity and the cavity stress response. However, recording sites at great depth are few, and most are located in granitic rock masses.

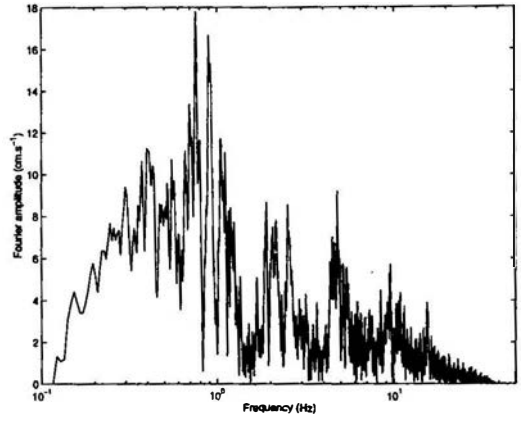

Figure 9: Fourier acceleration amplitude of the earthquake used for Fig.8

Obviously, damages such as the compressional rupture of reinforced concrete lining cannot be explained by the SH-wave study; compressional stress appears in SV- or P-wave analysis. Furthermore, in some cases, the hypothesis of the half-space is required. Thus, the concepts mentioned above are also defined for SV- and P-waves, as well as for the problems of half-space and lined structures. These were developed in ref.(Kurose 2000).

Finally, the stress response spectrum may provide engineers the order of magnitude of earthquake-related mechanical effects in an underground structure for a given motion and, conversely, for a given target *SRS*, may assist in producing a design earth-

quake more suitable for analysis of deep underground structures than those currently available.

8 ACKNOWLEDGEMENT

The writers gratefully acknowledge the financial support provided by the French National Radioactive Waste Management Agency (ANDRA) and Géostock. The writers would also like to thank Kazuhiro Aoki and Makoto Kawamura, Japan Nuclear Cycle Research Institute, for providing us with the ground-motion data, Prof. Shunsuke Sakurai, Director of the Hiroshima Institute of Technology, and Dr. Alain Pecker, Géodynamique et Structure. Many thanks go to Dr. Yoshimitsu Fukushima, Izumi Research Institute, Shimizu Construction, for advising Ayumi Kurose's research project.

REFERENCES

Betbeder-Matibet, J. (1999). L'atténuation des mouvements sismiques en profondeur. In *Génie Parasismique et Réponse Dynamique des Ouvrages. 5e Colloque National AFPS.*

Kawashima, K. (Ed.) (1994, April). *Earthquake-resistant design of underground structures (in Japanese).* Kajima Publishing Association.

Kurose, A. (2000). *Earthquake-related effects on underground structures (in French, summary in English).* PhD dissertation (to be defended in september 2000), Ecole Polytechnique, Palaiseau, France.

Pao, Y.-H. & Mow, C.-C. (1973). *Diffraction of Elastic Waves and Dynamic Stress Concentrations.* Crane, Russak and Co. Inc., ISBN 0-8448-0155-0.

Rathje, E., Abrahamson, N., & Bray, J. (1998, February). Simplified frequency content estimates of earthquake ground motion with a single parameter. *J. Geotech. and Geoenviron. Eng 124*(2).

Sakurai, S. (1995, November). Damage to tunnels due to the earthquake and relation to location of active faults (in Japanese). In *Special Issue on the 1995 Hanshin Awaji Great Earthquake.* Construction Engineering Research Institute Foundation.